SIAM J. SCI. COMPUT.
Vol. 19, No. 5, pp. 1646–1666, September 1998
© 1998 Society for Industrial and Applied Mathematics
014

FLEXIBLE MULTIPLE SEMICOARSENING FOR THREE-DIMENSIONAL SINGULARLY PERTURBED PROBLEMS*

T. WASHIO† AND C. W. OOSTERLEE‡

Abstract. We present robust parallel multigrid-based solvers for 3D scalar partial differential equations. The robustness is obtained by combining multiple semicoarsening strategies, matrix-dependent transfer operators, and a Krylov subspace acceleration. The basis for the 3D preconditioner is a 2D method with multiple semicoarsened grids based on the MG-S method from [C. W. Oosterlee, *Appl. Numer. Math.*, 19(1995), pp. 115–128] and [T. Washio and C. W. Oosterlee, GMD Arbeitspapier 949, GMD, St. Augustin, Germany, 1995]. The 2D method is generalized to three dimensions with a line smoother in the third dimension. The method based on semicoarsening has been parallelized with the grid partitioning technique [J. Linden, B. Steckel, and K. Stüben, *Parallel Comput.*, 7(1988), pp. 461–475], [O. A. McBryan et al., *Impact Comput. Sci. Engrg.*, 3(1991), pp. 1–75] and is evaluated as a solver and as a preconditioner on a MIMD machine. The robustness of the 3D method is shown for finite volume and finite difference discretizations of 3D anisotropic diffusion equations and convection-dominated convection-diffusion problems.

Key words. 3D solver, Krylov methods, multigrid preconditioner, flexible semicoarsening, robustness, parallel computing, grid partitioning

AMS subject classifications. 65N55, 65F10, 65Y05

PII. S1064827596305829

1. Introduction.

The goal of this paper is to find robust and parallel efficient solution methods for three-dimensional (3D) linear partial differential equations. Our starting point is a structured block diagonal matrix resulting from finite volume or finite difference discretizations of singularly perturbed problems. For the 3D problems we want to present an alternative to the use of alternating plane smoothers. Alternating plane smoothers are known to be robust smoothers in standard multigrid algorithms but they are expensive, because in every plane a sparse system of linear equations has to be solved. An alternative for avoiding this is to consider nonstandard multigrid methods. These methods involve a combination of local (point or line) smoothers and a robust coarse grid correction based on semicoarsened grids. Combining two-dimensional (2D) multiple semicoarsening and line smoothing with respect to the third dimension, a robust $O(N)$ solver is obtained. The resulting 3D solver is robust for a large class of problems.

It was found in analyzing the spectra in [17] that for all test problems, many of the eigenvalues of a multigrid iteration matrix are clustered around the origin. In some cases there are some isolated large eigenvalues which limit the multigrid convergence, but are captured nicely by a Krylov acceleration technique. A similar observation was made in [9] and [22]. Furthermore, the use of a (nonstandard) multigrid preconditioner for a Krylov method, with a fixed smoother and fixed transfer operators, leads to a well-parallelizable method.

One could develop for each of the problems treated here a specific optimized

*Received by the editors June 28, 1996; accepted for publication (in revised form) December 16, 1996; published electronically April 28, 1998.
http://www.siam.org/journals/sisc/19-5/30582.html
†C&C Research Laboratories, NEC Europe Ltd., Rathausallee 10, D-53757 Sankt Augustin, Germany (washio@ccrl-nece.technopark.gmd.de).
‡GMD, Institute for Algorithms and Scientific Computing, Schloss Birlinghoven, D-53754 Sankt Augustin, Germany (oosterlee@gmd.de).

multigrid solver. This is not our intention with this paper. We would also like to mention that algebraic multigrid (AMG) [19] is an interesting solver for some problems treated here. However, the approach presented is expected to be easy to generalize to systems of equations and nonlinear problems. AMG may be restricted in this respect, and also with respect to parallelism and locality.

The basis for the 3D solver is a 2D nonstandard multigrid method MG-S [15], [25], based on multiple semicoarsening. In 2D methods based on semicoarsening a point smoother is sufficient for achieving robustness. In [15] we explained the relation between our multiple semicoarsening approach and the use of a semicoarsened multigrid method as a smoother in a multigrid method with a standard grid sequence. MG-S is based on the standard multigrid grid sequence, and transfer operators with semicoarsened grids are only connected with at most one of these grids. Processing the semicoarsened grids can then be seen as the smoothing iteration in the standard grid sequence.

The 3D solution method based on the 2D flexible MG-S grid sequence with a line smoother in the third direction is explained in section 2. The 3D prolongation operators are based on de Zeeuw's [27] and Dendy's [2] 2D prolongation weights and Galerkin coarse grid discretization [26]. A V-cycle is used in the semicoarsening smoother. A V- and an F-cycle are implemented for the standard grid sequence. We evaluate whether the use of an F-cycle instead of a V-cycle accelerates the convergence with MG-S and if this acceleration outweighs the more frequent processing of the coarser grids.

In section 2.4 we present a more efficient *flexible* MG-S method. It is possible to construct a faster MG-S method, in which the fine and coarse grid matrices are analyzed and the semicoarsening in the smoother is stopped when anisotropies have disappeared.

Multiple coarse grids are also considered in the frequency domain decomposition method [7], [4] and in the multiple semicoarsened grids (MSG) method from [12], [13], [14], and [28]. Early multigrid work in which semicoarsening plays an important role is [18], where the multigrid reduction (MGR) method is introduced, [24], where robust 3D multigrid methods for Poisson-type equations are considered, and [23], where semicoarsening is investigated on a multiple instruction, multiple data (MIMD) machine.

The parallelization of the 3D method is based on grid partitioning and on the parallelization of a line relaxation method, as explained in [25]. The parallelization is done with the message-passing interface (MPI). It has been ensured that the single-block convergence is identical to the multiblock convergence. The new 3D flexible MG-S method introduced is compared as a solver and a preconditioner in section 3. Representative 3D anisotropic diffusion- and convection-dominated test problems are implemented and solved on the NEC Cenju-3 MIMD machine [8]. A well-known 3D test problem is the anisotropic diffusion equation [3], [24], [5], where the anisotropy is along one or two coordinate directions. The convection-dominated problems solved are convection-diffusion equations with spherical and cylindrical solutions.

2. The 3D solution method. The right preconditioned system to solve is:

$$AK^{-1}(K\phi) = f. \tag{1}$$

A is a matrix constructed from a 3D 27-point stencil in general. K^{-1} never has to be solved explicitly; instead, one iteration of a multilevel preconditioner, which will be explained in the following subsections, is performed. The Krylov subspace method

used for solving (1) is GMRES(m) [20]. The multilevel preconditioner will also be used as a solver based on a matrix splitting as follows:

$$K\phi^{(l+1)} + (A - K)\phi^{(l)} = f. \tag{2}$$

This is a usual repeated application of the multilevel solver. We call this Richardson iteration.

2.1. Basic idea of the 3D solution method. A first robust semicoarsening multigrid method with an F-cycle of complexity $O(N)$, with N the number of unknowns, was published in [12], where the MSG method was introduced. In [13] and [14], however, it was shown that it is not at all trivial to find satisfactory coarse grid corrections for MSG. A new variant, 2D MG-S, was discussed in [15] and [25]. The behavior of this method is clearer than that of MSG, because standard multigrid serves as a basis for this nonstandard multigrid method. The smoother investigated in the standard multigrid sequence is a semicoarsened multigrid method in the x- and y-directions. It is possible to present 2D MG-S as a standard multigrid method with an alternating semicoarsened multigrid smoother. A 2D standard multigrid for four levels is shown in Figure 1(a); the sequence of grids processed in MG-S is presented in Figure 1(b).

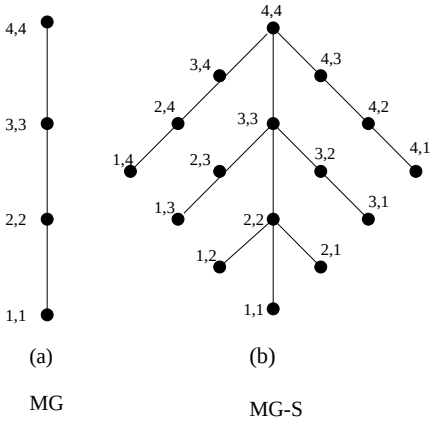

FIG. 1. *Sequences of* 2*D grids,* (a) *for standard multigrid,* (b) *for the MG-S method.*

A 2D MG-S cycle is performed as follows: first semicoarsening in the x-direction takes place with smoothing on all x-semicoarsened grids. After this, the semicoarsening in the y-direction is performed with smoothing on all grids. Then, a grid coarsened simultaneously in the x- and y-directions is processed. On this coarser grid level the same procedure takes place, and so on.

A robust 3D solution method is presented in this section, based on the 2D MG-S preconditioner with a line smoother in the third direction. This generalization seems to be a good compromise between storage and computational work. Storage would be less in methods based on the standard multigrid sequence in three dimensions. However, alternating plane smoothers would be required for robustness [24], [5], which are more expensive. In [5] one V-cycle of a 2D multigrid method was used as a plane smoother for solving 3D anisotropic diffusion equations with strong couplings in two directions simultaneously, in order to keep the plane smoother cheap. It cannot, however, be expected that one iteration of a plane smoother is generally sufficient

for more difficult convection-dominated equations. In [16] a plane smoother based on incomplete LU (ILU) preconditioned generalized minimum residual (GMRES) [21] leads to a robust multigrid method for 3D incompressible Navier–Stokes equations on stretched grids. It was found that for high Reynolds flows on fine grids the number of GMRES plane iterations increased in several planes. This phenomenon can lead to unbalanced workload on MIMD machines.

A full 3D MG-S or MSG method, where enough grids are processed so that even a point smoother gives a robust method, would need much more storage and computation.

2.2. Fourier smoothing analysis for the 3D MG-S. Our 3D variant is based on the following consideration for the Fourier smoothing analysis of a line smoother and the robustness of the 2D MG-S with a point smoother. First, we see that the convergence factor of a line smoother for a Fourier component depends essentially only on the frequencies along two directions perpendicular to the line. As in [1], suppose we are interested in solving the diffusion equation

$$L\phi(x,y,z) = a\frac{\partial^2\phi(x,y,z)}{\partial x^2} + b\frac{\partial^2\phi(x,y,z)}{\partial y^2} + c\frac{\partial^2\phi(x,y,z)}{\partial z^2} = f(x,y,z), \tag{3}$$

with positive coefficients a, b, and c. This equation can be discretized on a grid $G(h_x,h_y,h_z) = \{(ih_x, jh_y, kh_z) \mid i,j,k \in N\}$ by the standard seven-point discretization. Suppose, for example, we apply the damped z-line Jacobi relaxation with the damping parameter $\omega(0 < \omega \le 1)$ to the discretized equation; then we obtain an iterative process

$$(L_z + D)\tilde{\phi}^{(l+1)} + (L_x + L_y)\phi^{(l)} = f, \tag{4}$$

$$\phi^{(l+1)} = \omega\tilde{\phi}^{(l+1)} + (1-\omega)\phi^{(l)}, \tag{5}$$

where

$$\begin{aligned}
(L_x\phi)_{i,j,k} &:= a\frac{\phi_{i+1,j,k} + \phi_{i-1,j,k}}{{h_x}^2},\\
(L_y\phi)_{i,j,k} &:= b\frac{\phi_{i,j+1,k} + \phi_{i,j-1,k}}{{h_y}^2},\\
(L_z\phi)_{i,j,k} &:= c\frac{\phi_{i,j,k+1} + \phi_{i,j,k-1}}{{h_z}^2},\\
(D\phi)_{i,j,k} &:= -2\left(\frac{a}{{h_x}^2} + \frac{b}{{h_y}^2} + \frac{c}{{h_z}^2}\right)\phi_{i,j,k},\\
(\phi_{i,j,k} &= \phi(ih_x, jh_y, kh_z)).
\end{aligned}$$

Assume ϕ is the solution of the discretized equation and $e^{(l)} = \phi^{(l)} - \phi$ is the error at the lth iteration; then from (4) and (5) we obtain

$$\frac{1}{\omega}(L_z + D)e^{(l+1)} = \left(\frac{1-\omega}{\omega}(L_z + D) - (L_x + L_y)\right)e^{(l)}. \tag{6}$$

If we put

$$e^{(l)} = A_\theta^{(l)} e^{i(\theta_x x/h_x + \theta_y y/h_y + \theta_z z/h_z)} \quad (\theta = (\theta_x, \theta_y, \theta_z)), \tag{7}$$

and substitute these error functions in (6), then we obtain

$$\begin{aligned}&\frac{2}{\omega}A_\theta^{(l+1)}\left(-\frac{a}{{h_x}^2}-\frac{b}{{h_y}^2}-(1-\cos\theta_z)\frac{c}{{h_z}^2}\right)\\&=2A_\theta^{(l)}\left(\frac{1-\omega}{\omega}\left(-\frac{a}{{h_x}^2}-\frac{b}{{h_y}^2}-(1-\cos\theta_z)\frac{c}{{h_z}^2}\right)-\cos\theta_x\frac{a}{{h_x}^2}-\cos\theta_y\frac{b}{{h_y}^2}\right).\end{aligned}\tag{8}$$

Hence the convergence factor [1] of the θ component is

$$\mu(\theta)=\left|\frac{A_\theta^{(l+1)}}{A_\theta^{(l)}}\right|=\frac{\left|((1-\omega)+\omega\cos\theta_x)a/{h_x}^2+((1-\omega)+\omega\cos\theta_y)b/{h_y}^2+(1-\omega)(1-\cos\theta_z)c/{h_z}^2\right|}{a/{h_x}^2+b/{h_y}^2+(1-\cos\theta_z)c/{h_z}^2}.\tag{9}$$

From the fact that

$$\left|\frac{B+\dot{B}}{A+\dot{A}}\right|\le\max\left(\left|\frac{B}{A}\right|,\left|\frac{\dot{B}}{\dot{A}}\right|\right)\ \text{for}\ A,\dot{A}>0\ \text{and}\ \forall B,\dot{B},\tag{10}$$

we obtain the following inequality for the convergence factor in (9):

$$\mu(\theta)\le\max\left(1-\omega,\mu_2(\theta_x,\theta_y)\right),\tag{11}$$

where

$$\mu_2(\theta_x,\theta_y)=\left|\frac{((1-\omega)+\omega\cos\theta_x)a/{h_x}^2+((1-\omega)+\omega\cos\theta_y)b/{h_y}^2}{a/{h_x}^2+b/{h_y}^2}\right|.\tag{12}$$

Here $\mu_2(\theta_x,\theta_y)$ in (12) is the convergence factor of the 2D damped point Jacobi relaxation for the operator $a\partial^2/\partial x^2+b\partial^2/\partial y^2$ on the grid $G(h_x,h_y)=\{(ix,jy)\mid i,j\in N\}$.

From this consideration, we see that if there is a 2D robust multigrid cycle with the damped point Jacobi relaxation for any positive coefficients a and b, we can realize a robust 3D solver by employing the damped z-line Jacobi relaxation combined with this 2D cycle for the x-y planes without coarsening the grids in the z-direction. Similar observations can be made for other 3D z-line relaxations.

For the 2D robust multigrid cycle with a point smoother, we employ the 2D MG-S cycle. The robustness of the 2D MG-S is explained as follows.

For multigrid it is well known that high frequency error components are reduced by a smoothing method, while low frequency components are reduced on coarse grids. In Fourier smoothing analysis the error between the numerical and the exact solutions, $e_h=\phi_h-\phi$, on the grid $G(h_x,h_y)$, is expressed as Fourier components in two dimensions as follows:

$$e_h=e^{i(\theta_x x/h_x+\theta_y y/h_y)}=e^{i(\hat{\theta}_x x+\hat{\theta}_y y)},\tag{13}$$

with $\theta=(\theta_x,\theta_y)=(\hat{\theta}_x h_x,\hat{\theta}_y h_y)$ and $h=(h_x,h_y)$. Here $\hat{\theta}$ corresponds to the representation of the Fourier components independent of the grid size. The representation by $\hat{\theta}$ is useful for looking at the convergence factors on various grids.

All Fourier components can be mapped on the visible components on $G(h_x,h_y)$ in $|\theta|:=\max(|\theta_x|,|\theta_y|)\le\pi$. For standard multigrid coarsening $G(h_x,h_y)\to G(2h_x,2h_y)$

high frequency error components correspond to the parts of the visible Fourier domain $\pi/2 \le |\theta| \le \pi$, while the low frequency components are located in the region $|\theta| < \pi/2$; see Figure 2(a). Since this high frequency domain is not visible on the coarse grid $G(2h_x, 2h_y)$, we should reduce all error components corresponding to the high frequency domain by the smoothing method on the fine grid $G(h_x, h_y)$. This is possible with a simple point smoother if the diffusion problem is not anisotropic. For example, the convergence factor of the damped point Jacobi relaxation $\mu_2(\theta_x, \theta_y)$ in (12) is bounded by

$$\mu_2(\theta_x, \theta_y) \le \frac{a/{h_x}^2 + \max(1-\omega, |1-2\omega|)b/{h_y}^2}{a/{h_x}^2 + b/{h_y}^2} \ \forall\theta_x,\ \pi/2 \le |\theta_y| \le \pi, \tag{14}$$

$$\mu_2(\theta_x, \theta_y) \le \frac{\max(1-\omega, |1-2\omega|)a/{h_x}^2 + b/{h_y}^2}{a/{h_x}^2 + b/{h_y}^2},\ \pi/2 \le |\theta_x| \le \pi\ \forall\theta_y. \tag{15}$$

In particular, the convergence factor is bounded on the high frequency region as follows:

$$\mu_2(\theta_x, \theta_y) \le \frac{A + \max(1-\omega, |1-2\omega|)}{A+1},\ \pi/2 \le |\theta| \le \pi, \tag{16}$$

where

$$A = \max\left(\left(\frac{a}{{h_x}^2}\right)/\left(\frac{b}{{h_y}^2}\right), \left(\frac{b}{{h_y}^2}\right)/\left(\frac{a}{{h_x}^2}\right)\right). \tag{17}$$

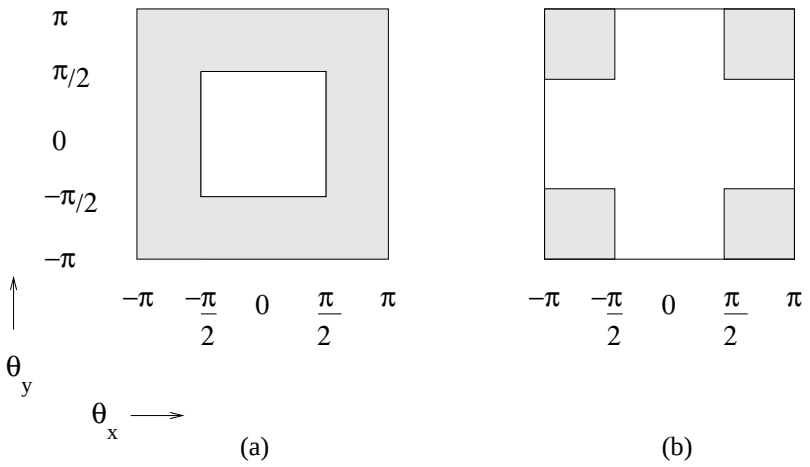

FIG. 2. *Error components in Fourier space:* (a) *standard multigrid high and low frequency regions,* (b) *the high frequency regions for both directions.*

Here we intend to construct an efficient smoothing method with point smoothers on semicoarsened grids which reduces the high frequency error components on $G(h_x, h_y)$ for any combination of the positive coefficients a and b. First we see that $\mu_2(\theta_x, \theta_y)$ is bounded away from 1 if both θ_x and θ_y are in the high frequency region. This region is depicted in Figure 2(b). From the inequality (10), we obtain

$$\mu_2(\theta_x, \theta_y) \le \max(1-\omega, |1-2\omega|),\ \pi/2 \le |\theta_x| \le \pi,\ \text{and}\ \pi/2 \le |\theta_y| \le \pi. \tag{18}$$

For convenience in the following explanation, we define four regions $R_1(h_x, h_y), \ldots, R_4(h_x, h_y)$ in the Fourier space with respect to the grid-independent parameter $\hat{\theta}$ for the grid $G(h_x, h_y)$ as follows:

$$
\begin{aligned}
R_1(h_x, h_y) &:= \{(\hat{\theta}_x, \hat{\theta}_y) \mid \pi/2 \le \max(|\hat{\theta}_x|h_x, |\hat{\theta}_y|h_y) \le \pi\},\\
R_2(h_x, h_y) &:= \{(\hat{\theta}_x, \hat{\theta}_y) \mid \pi/2 \le |\hat{\theta}_x|h_x \le \pi, \pi/2 \le |\hat{\theta}_y|h_y \le \pi\},\\
R_3(h_x, h_y) &:= \{(\hat{\theta}_x, \hat{\theta}_y) \mid \pi/2 \le |\hat{\theta}_y|h_y \le \pi\},\\
R_4(h_x, h_y) &:= \{(\hat{\theta}_x, \hat{\theta}_y) \mid \pi/2 \le |\hat{\theta}_x|h_x \le \pi\}.
\end{aligned}
$$

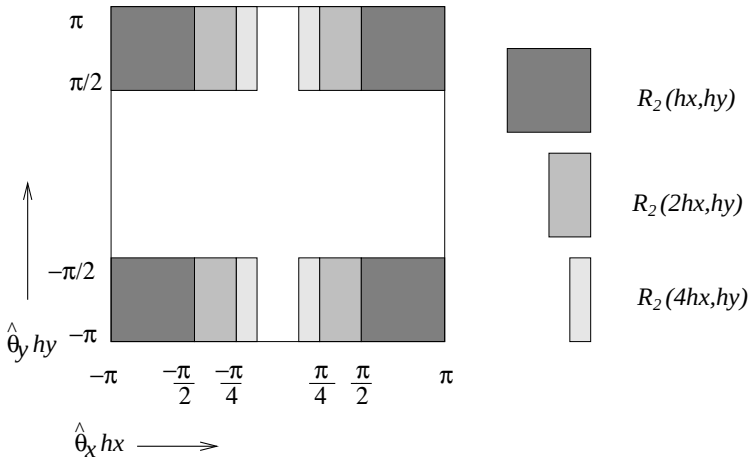

FIG. 3. *Grid-independent representation of error components of Fourier space.*

By using these regions, the idea to reduce high frequency error components on $G(h_x, h_y)$ is explained as follows. From the above definition, $R_1(h_x, h_y)$ corresponds to the high frequency region of the grid $G(h_x, h_y)$. $R_2(h_x, h_y)$ is a region where the inequality (18) is valid. $R_1(h_x, h_y)$ is covered by $R_3(h_x, h_y)$ and $R_4(h_x, h_y)$. The error components corresponding to $R_3(h_x, h_y)$ can be efficiently reduced by combining the point relaxations on the grids $G(h_x, h_y)$, $G(2h_x, h_y)$, $G(4h_x, h_y)$, ..., since $R_3(h_x, h_y)$ is covered by $R_2(h_x, h_y)$, $R_2(2h_x, h_y)$, $R_2(4h_x, h_y)$, ... (see Figure 3), and the error components corresponding to $R_2(2^l h_x, h_y)$ are efficiently reduced by the point relaxation on $G(2^l h_x, h_y)$ from (18). This is done by a semicoarsened V-cycle along the x-direction in the 2D MG-S. For the same reason, a semicoarsened V-cycle along the y-direction is employed in order to reduce the error components corresponding to $R_4(h_x, h_y)$. Namely, in the 2D MG-S the alternating semicoarsened V-cycle is used as a smoother on the standard grid sequence.

From the inequalities (14) and (15), we see that we do not have to employ all semicoarsened grids. For example, it would be enough to continue the x-semicoarsening until $a/(2^l h_x)^2$ is in the same order of magnitude as $b/{h_y}^2$ (or smaller). This observation motivates us to construct a flexible semicoarsening according to the strength of the anisotropy. The criteria to stop the semicoarsenings are proposed in section 2.4.

It should be mentioned here that the 3D method is not invariant with respect to rotation of the axes. However, numerical experiments show that the sensitivity of the convergence for the rotation of the axes is small in most cases, as can be observed in the results for the anisotropic diffusion equation in section 3.

2.3. Components of the 3D solution method. The different grids in a full 3D MG-S method are now described. Only two superindices are needed, since the number of grid points in the z-direction is fixed.

First, the grids coarsened in the x- and y-directions simultaneously, G^{m_x,m_y}, $G^{m_x-1,m_y-1},\ldots,G^{1,m_y-m_x+1}$ (or $G^{m_x-m_y+1,1}$), are constructed according to:

$$G^{m_x,m_y} = G, \tag{19}$$

$$G^{m_x-l,m_y-l} = \{(i,j,k)|(2i-1,2j-1,k) \in G^{m_x-l+1,m_y-l+1}\},$$

$$1 \le l \le \min(m_x,m_y)-1. \tag{20}$$

Then, on each grid level, semicoarsening takes place sequentially in two directions:

$$G^{m_x-l-l_x,m_y-l} := \{(i,j,k) \mid (2i-1,j,k) \in G^{m_x-l-l_x+1,m_y-l}\}; 1 \le l_x \le m_x-l-1,$$
$$G^{m_x-l,m_y-l-l_y} := \{(i,j,k) \mid (i,2j-1,k) \in G^{m_x-l,m_y-l-l_y+1}\}; 1 \le l_y \le m_y-l-1.$$

Figure 4 shows a picture of three levels of the full 3D MG-S method with the connections between the grids.

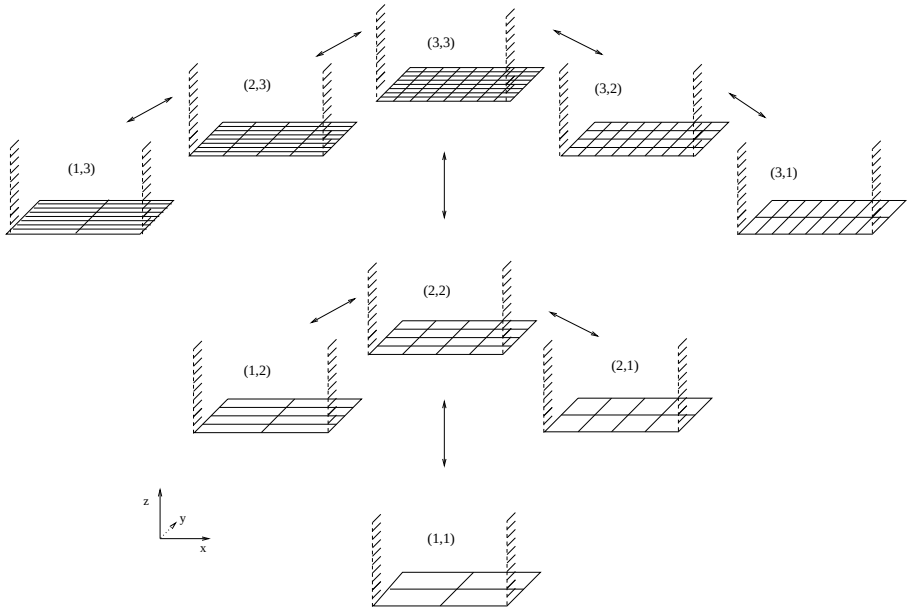

FIG. 4. *The full 3D MG-S method with grid indices (l_x,l_y) with various semicoarsenings in the x- and y-directions with a line smoother in the z-direction.*

Transfer and coarse grid operators. The transfer operators between the different grids are combinations of earlier-defined prolongation and restriction mappings [25], [17]. Along the standard multigrid sequence of 2D MG-S in [25], the prolongation operators were based on the weights from [2], as were the prolongation weights between the semicoarsened grids. In [17], however, it was found that the performance of standard multigrid with the upwind prolongation weights from [27] resulted in better convergence for convection-dominated convection-diffusion problems. These weights (explained in detail in [27], [26], and [17]) are also used here along the (x,y)-coarsened

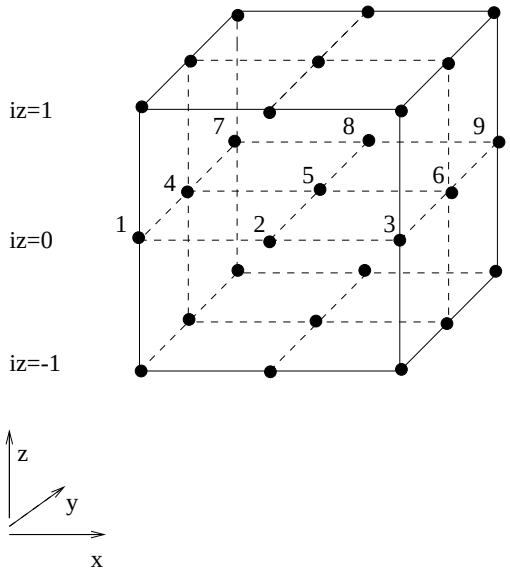

FIG. 5. *The 27-point stencil with numbering.*

grid sequence. (We define "(x,y)-coarsened" here as coarsening in the x- and y-directions simultaneously.) Along the semicoarsened grids the transfer operators from [25], based on [2], are most natural and resulted in the best convergence.

The 3D weights are now explained. Assuming we have the following 27-point stencil matrix on a grid G^{l_x,l_y}:

$$
\begin{aligned}
&(A\phi)_{i,j,k} \\
&= \sum_{iz=-1,0,1} (a(iz)^1_{i,j,k}\phi_{i-1,j-1,k+iz} + a(iz)^2_{i,j,k}\phi_{i,j-1,k+iz} + a(iz)^3_{i,j,k}\phi_{i+1,j-1,k+iz} \\
&\quad + a(iz)^4_{i,j,k}\phi_{i-1,j,k+iz} + a(iz)^5_{i,j,k}\phi_{i,j,k+iz} + a(iz)^6_{i,j,k}\phi_{i+1,j,k+iz} \\
&\quad + a(iz)^7_{i,j,k}\phi_{i-1,j+1,k+iz} + a(iz)^8_{i,j,k}\phi_{i,j+1,k+iz} + a(iz)^9_{i,j,k}\phi_{i+1,j+1,k+iz}).
\end{aligned} \tag{21}
$$

Figure 5 shows the 27-point stencil with numbering.

We define a lumped 9-point stencil matrix $\tilde{A}$ in an (x,y)-plane as:

$$
\begin{aligned}
(\tilde{A}\phi)_{i,j,k} = {} & \tilde{a}^1_{i,j,k}\phi_{i-1,j-1,k} + \tilde{a}^2_{i,j,k}\phi_{i,j-1,k} + \tilde{a}^3_{i,j,k}\phi_{i+1,j-1,k} \\
& + \tilde{a}^4_{i,j,k}\phi_{i-1,j,k} + \tilde{a}^5_{i,j,k}\phi_{i,j,k} + \tilde{a}^6_{i,j,k}\phi_{i+1,j,k} \\
& + \tilde{a}^7_{i,j,k}\phi_{i-1,j+1,k} + \tilde{a}^8_{i,j,k}\phi_{i,j+1,k} + \tilde{a}^9_{i,j,k}\phi_{i+1,j+1,k}
\end{aligned} \tag{22}
$$

with

$$
\tilde{a}^p_{i,j,k} = a(-1)^p_{i,j,k} + a(0)^p_{i,j,k} + a(1)^p_{i,j,k},\ p = 1, 2, \ldots, 9. \tag{23}
$$

With the lumped matrix $\tilde{A}$, we define the weights $w1, \ldots, w4$ of the following prolongations.

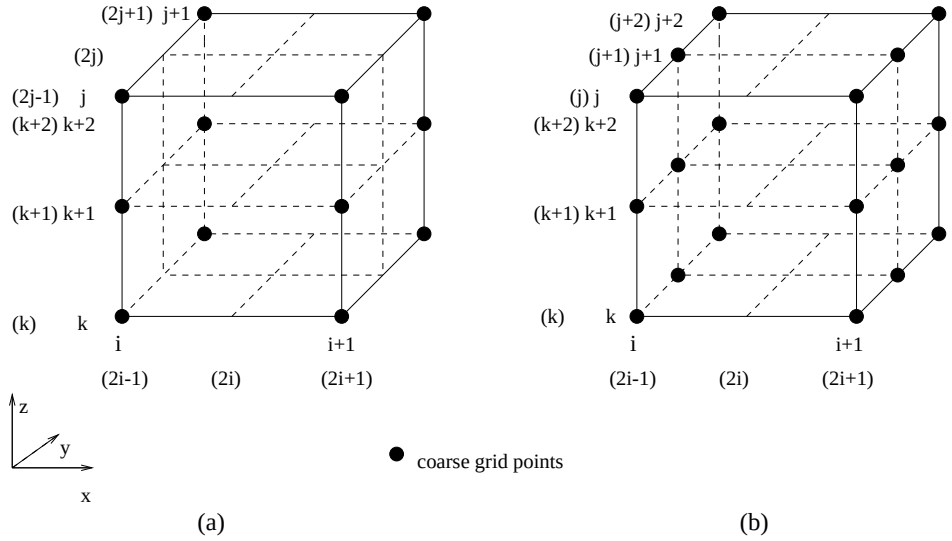

FIG. 6. (a) *Two coarse grid cells and eight fine grid cells for semicoarsening in the x- and y-directions.* (b) *Four coarse grid cells and eight fine grid cells for x-semicoarsening. (The fine grid indices are in brackets; the coarse grid indices are not.)*

$$P^{l_x,l_y} : u \in Q^{G^{l_x-1,l_y-1}} \mapsto v \in Q^{G^{l_x,l_y}} \quad :$$

$$v_{2i-1,2j-1,k} = u_{i,j,k}, \tag{24}$$

$$v_{2i,2j-1,k} = w1_{2i,2j-1,k}u_{i,j,k} + w2_{2i,2j-1,k}u_{i+1,j,k}, \tag{25}$$

$$v_{2i-1,2j,k} = w1_{2i-1,2j,k}u_{i,j,k} + w3_{2i-1,2j,k}u_{i,j+1,k}, \tag{26}$$

$$\begin{aligned} v_{2i,2j,k} = {} & w1_{2i,2j,k}u_{i,j,k} + w2_{2i,2j,k}u_{i+1,j,k} \\ & + w3_{2i,2j,k}u_{i,j+1,k} + w4_{2i,2j,k}u_{i+1,j+1,k}. \end{aligned} \tag{27}$$

$$P_x^{l_x,l_y} : u \in Q^{G^{l_x-1,l_y}} \mapsto v \in Q^{G^{l_x,l_y}} \quad :$$

$$v_{2i-1,j,k} = u_{i,j,k}, \tag{28}$$

$$v_{2i,j,k} = w1_{2i,j,k}u_{i,j,k} + w2_{2i,j,k}u_{i+1,j,k}. \tag{29}$$

$$P_y^{l_x,l_y} : u \in Q^{G^{l_x,l_y-1}} \mapsto v \in Q^{G^{l_x,l_y}} \quad :$$

$$v_{i,2j-1,k} = u_{i,j,k}, \tag{30}$$

$$v_{i,2j,k} = w1_{i,2j,k}u_{i,j,k} + w3_{i,2j,k}u_{i,j+1,k}. \tag{31}$$

Figure 6 shows coarse and fine grid cells for (x,y)- and x-coarsening.

In order to construct the prolongation operator P^{m_x-l,m_y-l}, the matrix $\tilde{A}$ is split into a symmetric and an antisymmetric part to obtain appropriate prolongation weights for the diffusion-dominated (symmetric) part and the convection-dominated (antisymmetric) part, as in [27]:

$$S = \frac{1}{2}(\tilde{A} + \tilde{A}^T), \;\; T = \tilde{A} - S = \frac{1}{2}(\tilde{A} - \tilde{A}^T). \tag{32}$$

The diagonal elements of matrices S and T are numbered similarly as the elements of $\tilde{A}$ in (22). We now define west, east, north, and south matrix-dependent quantities from the symmetric part:

$$
\begin{aligned}
d_w &= \max(|s^1_{2i,2j-1,k} + s^4_{2i,2j-1,k} + s^7_{2i,2j-1,k}|, |s^1_{2i,2j-1,k}|, |s^7_{2i,2j-1,k}|),\\
d_e &= \max(|s^3_{2i,2j-1,k} + s^6_{2i,2j-1,k} + s^9_{2i,2j-1,k}|, |s^3_{2i,2j-1,k}|, |s^9_{2i,2j-1,k}|),\\
d_n &= \max(|s^7_{2i-1,2j,k} + s^8_{2i-1,2j,k} + s^9_{2i-1,2j,k}|, |s^7_{2i-1,2j,k}|, |s^9_{2i-1,2j,k}|),\\
d_s &= \max(|s^1_{2i-1,2j,k} + s^2_{2i-1,2j,k} + s^3_{2i-1,2j,k}|, |s^1_{2i-1,2j,k}|, |s^3_{2i-1,2j,k}|),\\
\sigma_1 &= \frac{1}{2}\min\left(1, \left|1 - \frac{\sum_{p=1}^9 s^p_{2i,2j-1,k}}{a^5_{2i,2j-1,k}}\right|\right),\\
\sigma_2 &= \frac{1}{2}\min\left(1, \left|1 - \frac{\sum_{p=1}^9 s^p_{2i-1,2j,k}}{a^5_{2i-1,2j}}\right|\right).
\end{aligned}
$$

Also, two quantities c_1 and c_2 for the antisymmetric part in the x- and y-directions are defined:

$$
\begin{aligned}
c_1 &= t^3_{2i,2j-1,k} + t^6_{2i,2j-1,k} + t^9_{2i,2j-1,k} - (t^1_{2i,2j-1,k} + t^4_{2i,2j-1,k} + t^7_{2i,2j-1,k}),\\
c_2 &= t^7_{2i-1,2j,k} + t^8_{2i-1,2j,k} + t^9_{2i-1,2j,k} - (t^1_{2i-1,2j,k} + t^2_{2i-1,2j,k} + t^3_{2i-1,2j,k}).
\end{aligned}
$$

With these quantities the matrix-dependent weights on the east, west, north, and south sides are constructed as follows:

$$
\begin{aligned}
w_w &= \sigma_1\left[1 + \frac{d_w - d_e}{d_w + d_e} + \frac{c_1}{d_w + d_e + d_n + d_s}\right],\\
w_e &= 2\sigma_1 - w_w,\\
w_n &= \sigma_2\left[1 + \frac{d_s - d_n}{d_s + d_n} + \frac{c_2}{d_w + d_e + d_n + d_s}\right],\\
w_s &= 2\sigma_2 - w_n.
\end{aligned}
$$

The weights $w1$ and $w2$ are now computed as:

- for $(2i, 2j-1, k) \in Q^{G^{m_x-l,m_y-l}}$,
$$w1_{2i,2j-1,k} = \min(2\sigma_1, \max(0, w_w)),\ w2_{2i,2j-1,k} = \min(2\sigma_1, \max(0, w_e));$$
- for $(2i-1, 2j, k) \in Q^{G^{m_x-l,m_y-l}}$,
$$w1_{2i-1,2j,k} = \min(2\sigma_2, \max(0, w_s)),\ w3_{2i-1,2j,k} = \min(2\sigma_2, \max(0, w_n));$$
- for $(2i, 2j, k) \in Q^{G^{m_x-l,m_y-l}}$,
$$
\begin{aligned}
w1_{2i,2j,k} &= (\tilde{a}^1_{2i,2j,k} + \tilde{a}^2_{2i,2j,k} \cdot w1_{2i,2j-1,k} + \tilde{a}^4_{2i,2j,k} \cdot w1_{2i-1,2j,k})/(\tilde{a}^5_{2i,2j,k}),\\
w2_{2i,2j,k} &= (\tilde{a}^3_{2i,2j,k} + \tilde{a}^2_{2i,2j,k} \cdot w2_{2i,2j-1,k} + \tilde{a}^6_{2i,2j,k} \cdot w1_{2i+1,2j,k})/(\tilde{a}^5_{2i,2j,k}),\\
w3_{2i,2j,k} &= (\tilde{a}^7_{2i,2j,k} + \tilde{a}^4_{2i,2j,k} \cdot w3_{2i-1,2j,k} + \tilde{a}^8_{2i,2j,k} \cdot w1_{2i,2j+1,k})/(\tilde{a}^5_{2i,2j,k}),\\
w4_{2i,2j,k} &= (\tilde{a}^9_{2i,2j,k} + \tilde{a}^6_{2i,2j,k} \cdot w3_{2i+1,2j,k} + \tilde{a}^8_{2i,2j,k} \cdot w2_{2i,2j+1,k})/(\tilde{a}^5_{2i,2j,k}).
\end{aligned}
$$

For the grid prolongation operator from $P_x^{m_x-l-l_x,m_y-l}$ the weights are given as:

- for $(2i, j, k) \in Q^{G^{m_x-l-l_x,m_y-l}}$,
$$
\begin{aligned}
w1_{2i,j,k} &= (-\tilde{a}^1_{i,j,k} - \tilde{a}^4_{i,j,k} - \tilde{a}^7_{i,j,k})/(\tilde{a}^2_{i,j,k} + \tilde{a}^5_{i,j,k} + \tilde{a}^8_{i,j,k}),\\
w2_{2i,j,k} &= (-\tilde{a}^3_{i,j,k} - \tilde{a}^6_{i,j,k} - \tilde{a}^9_{i,j,k})/(\tilde{a}^2_{i,j,k} + \tilde{a}^5_{i,j,k} + \tilde{a}^8_{i,j,k}).
\end{aligned}
$$

For the grid prolongation operator from $P_y^{m_x-l,m_y-l-l_y}$ the weights are defined as:

- for $(i, 2j, k) \in Q^{G^{m_x-l,m_y-l-l_y}}$,
$$
\begin{aligned}
w1_{i,2j,k} &= (-\tilde{a}^1_{i,j,k} - \tilde{a}^2_{i,j,k} - \tilde{a}^3_{i,j,k})/(\tilde{a}^4_{i,j,k} + \tilde{a}^5_{i,j,k} + \tilde{a}^6_{i,j,k}),\\
w3_{i,2j,k} &= (-\tilde{a}^7_{i,j,k} - \tilde{a}^8_{i,j,k} - \tilde{a}^9_{i,j,k})/(\tilde{a}^4_{i,j,k} + \tilde{a}^5_{i,j,k} + \tilde{a}^6_{i,j,k}).
\end{aligned}
$$

For some difficult problems, negative values are observed in $w1, w2, w3$ even if the matrix on the finest grid G^{m_x,m_y} is an M-matrix. The negative weights make a

coarse grid matrix less diagonally dominant. This sometimes results in divergence of the relaxation on the coarser grid. In order to avoid this, we adopt a lumping procedure to keep nonnegative weights $w1, w2, w3$. In our experiments, we observe that this procedure improves the convergence and prevents the divergence of MG-S as a solver. If, for example, $w1_{i,2j,k}$ or $w3_{i,2j,k}$ is negative, we lump all positive off-diagonal elements $\tilde{a}^{p}_{i,2j,k}$ with the main diagonal element $\tilde{a}^{5}_{i,2j,k}$ and recompute the weights from the lumped matrix.

With the prolongation P^{m_x-l,m_y-l} defined along the (x,y)-coarsened grids, the restriction $R^{m_x-l,m_y-l} : v \in Q^{G^{m_x-l,m_y-l}} \mapsto u \in Q^{G^{m_x-l-1,m_y-l-1}}$ is defined as:

$$R^{m_x-l,m_y-l} = \left(P^{m_x-l,m_y-l}\right)^T,\ 0 \le l \le \min(m_x, m_y) - 2. \tag{33}$$

With $P_x^{m_x-l-l_x,m_y-l}$ as the prolongation along x-semicoarsened grids, the restriction mapping $R_x^{m_x-l-l_x,m_y-l} : Q^{G^{m_x-l-l_x,m_y-l}} \mapsto Q^{G^{m_x-l-l_x-1,m_y-l}}$ is defined as the transpose of $P_x^{m_x-l-l_x,m_y-l}$:

$$R_x^{m_x-l-l_x,m_y-l} = \left(P_x^{m_x-l-l_x,m_y-l}\right)^T. \tag{34}$$

The transfer operators along y-semicoarsened grids are constructed similarly. The coarse grid matrices A^{m_x-l,m_y-l} on (x,y)-coarsened grids G^{m_x-l,m_y-l} are defined with the Galerkin coarse grid approximation [6], [26], [27], [25]:

$$A^{m_x,m_y} = A, \tag{35}$$

$$A^{m_x-l-1,m_y-l-1} = R^{m_x-l,m_y-l} A^{m_x-l,m_y-l} P^{m_x-l,m_y-l}, \quad 0 \le l \le \min(m_x, m_y) - 2. \tag{36}$$

Along the semicoarsened grids the matrices are defined as:

$$A^{m_x-l-l_x-1,m_y-l} := R_x^{m_x-l-l_x,m_y-l} A^{m_x-l-l_x,m_y-l} P_x^{m_x-l-l_x,m_y-l}, \quad 0 \le l_x \le m_x - l - 2, \tag{37}$$

$$A^{m_x-l,m_y-l-l_y-1} := R_y^{m_x-l,m_y-l-l_y} A^{m_x-l,m_y-l-l_y} P_y^{m_x-l,m_y-l-l_y}, \quad 0 \le l_y \le m_y - l - 2. \tag{38}$$

2.4. Flexible MG-S cycle. It is not necessary to process all grids for all problems, as one can imagine from the inequalities (14) and (15). For several model problems it is not necessary to process the semicoarsened grids at all, as excellent convergence would be obtained. In the flexible MG-S method semicoarsening (from G^{l_x,l_y} to G^{l_x-1,l_y} or from G^{l_x,l_y} to G^{l_x,l_y-1}) is stopped as soon as no strong couplings along the semicoarsened direction are detected in the matrix $\tilde{A}$. In the case of semicoarsening along the x-direction, a criterion for detection is constructed as follows. The symmetric part of the matrix, $S = \frac{1}{2}(\tilde{A} + \tilde{A}^T)$, is used to detect strong coupling of unknowns from anisotropic diffusion. The criterion is based on the parameter $\mathrm{dif}^x_{i,j}$, defined as

$$\mathrm{dif}^x_{i,j} = \max_k \left\{ \frac{-s^4_{i,j,k} - s^6_{i,j,k}}{\tilde{a}^5_{i,j,k}} \right\}. \tag{39}$$

In order to detect strong coupling of unknowns from convection dominance we define $\mathrm{cnv}^{x(-)}_{i,j}$ and $\mathrm{cnv}^{x(+)}_{i,j}$ from the matrix $\tilde{A}$:

$$\mathrm{cnv}_{i,j}^{x(-)} = \max_k \left\{ \frac{-\tilde{a}_{i,j,k}^4}{\tilde{a}_{i,j,k}^5} \right\}, \tag{40}$$

$$\mathrm{cnv}_{i,j}^{x(+)} = \max_k \left\{ \frac{-\tilde{a}_{i,j,k}^6}{\tilde{a}_{i,j,k}^5} \right\}. \tag{41}$$

Semicoarsening in the x-direction continues if for some (i,j) one of the following conditions is fulfilled:

$$\mathrm{dif}_{i,j}^x > \delta_1 \text{ and } \mathrm{dif}_{i+1,j}^x > \delta_1, \tag{42}$$

$$\mathrm{cnv}_{i,j}^{x(-)} > \delta_2 \text{ and } \mathrm{cnv}_{i+1,j}^{x(-)} > \delta_2, \tag{43}$$

$$\mathrm{cnv}_{i,j}^{x(+)} > \delta_2 \text{ and } \mathrm{cnv}_{i+1,j}^{x(+)} > \delta_2. \tag{44}$$

A proper choice for the parameters δ_i is very important for robustness and efficiency. The choice can even depend on the smoother used. Satisfactory values for δ_i are chosen as: $\delta_1 = \delta_2 = 0.6$.

The criteria for the y-directions can be derived in a similar way. With these criteria it is possible that semicoarsening does not take place at all, so that the standard grid sequence is processed, or that only semicoarsening along one direction is applied.

MG-S algorithm. A 3D MG-S F-cycle algorithm with an alternating semicoarsened V-cycle as a smoother will be given here. Along with the number of pre- and postsmoothing steps along the (x,y)-coarsened grids, which are denoted by (ν_1, ν_2), the number of pre- and postsmoothing steps in the V-cycle semicoarsening smoother, denoted by (μ_1, μ_2), can also be varied. Our $\mathrm{F}(\nu_1,\nu_2)^{(\mu_1,\mu_2)}$ algorithm can be described as follows:

$\mathrm{F}(\nu_1,\nu_2)^{(\mu_1,\mu_2)}(A^{l_x,l_y}, f^{l_x,l_y}, \phi^{l_x,l_y}, \nu_1, \nu_2)$ {
  if ($l_x = 1$ or $l_y = 1$) {
    for $it = 1, \ldots, \nu_1 + \nu_2$
      $\phi^{l_x,l_y} := \mathrm{V}_x(A^{l_x,l_y}, f^{l_x,l_y}, \phi^{l_x,l_y}, \mu_1, \mu_2)$;
      $\phi^{l_x,l_y} := \mathrm{V}_y(A^{l_x,l_y}, f^{l_x,l_y}, \phi^{l_x,l_y}, \mu_1, \mu_2)$;
    end ;
    return ;
  } ;
  for $it = 1, \ldots, \nu_1$
    $\phi^{l_x,l_y} := \mathrm{V}_x(A^{l_x,l_y}, f^{l_x,l_y}, \phi^{l_x,l_y}, \mu_1, \mu_2)$;
    $\phi^{l_x,l_y} := \mathrm{V}_y(A^{l_x,l_y}, f^{l_x,l_y}, \phi^{l_x,l_y}, \mu_1, \mu_2)$;
  end ;
  $r^{l_x,l_y} := f^{l_x,l_y} - A^{l_x,l_y}\phi^{l_x,l_y}$;
  $f^{l_x-1,l_y-1} := R^{l_x,l_y} r^{l_x,l_y}$;
  $\phi^{l_x-1,l_y-1} := 0$;
  $\mathrm{F}(\nu_1,\nu_2)^{(\mu_1,\mu_2)}(A^{l_x-1,l_y-1}, f^{l_x-1,l_y-1}, \phi^{l_x-1,l_y-1}, \nu_1, \nu_2)$;
  $\phi^{l_x,l_y} := \phi^{l_x,l_y} + P^{l_x,l_y}\phi^{l_x-1,l_y-1}$;
  for $it = 1, \ldots, \nu_2$
    $\phi^{l_x,l_y} := \mathrm{V}_x(A^{l_x,l_y}, f^{l_x,l_y}, \phi^{l_x,l_y}, \mu_1, \mu_2)$;
    $\phi^{l_x,l_y} := \mathrm{V}_y(A^{l_x,l_y}, f^{l_x,l_y}, \phi^{l_x,l_y}, \mu_1, \mu_2)$;
  end ;
  (if this is the finest grid) return ;
  $r^{l_x,l_y} = f^{l_x,l_y} - A^{l_x,l_y}\phi^{l_x,l_y}$;
  $f^{l_x-1,l_y-1} := R^{l_x,l_y} r^{l_x,l_y}$;

$\phi^{l_x-1,l_y-1} := 0;$
$\mathrm{V}(\nu_1,\nu_2)^{(\mu_1,\mu_2)}(A^{l_x-1,l_y-1}, f^{l_x-1,l_y-1}, \phi^{l_x-1,l_y-1}, \nu_1, \nu_2);$
$\phi^{l_x,l_y} := \phi^{l_x,l_y} + P^{l_x,l_y}\phi^{l_x-1,l_y-1};$
for $it = 1, ..., \nu_2$
$\phi^{l_x,l_y} := \mathrm{V}_x(A^{l_x,l_y}, f^{l_x,l_y}, \phi^{l_x,l_y}, \mu_1, \mu_2);$
$\phi^{l_x,l_y} := \mathrm{V}_y(A^{l_x,l_y}, f^{l_x,l_y}, \phi^{l_x,l_y}, \mu_1, \mu_2);$
end ;
}

Here $\mathrm{V}(\nu_1,\nu_2)^{(\mu_1,\mu_2)}$ represents the MG-S V-cycle with an alternating semicoarsened V-cycle as a smoother. This is defined similarly to the F-cycle above. Note that in our F-cycle postsmoothing is done more often than presmoothing, since on intermediate grids after a prolongation, postsmoothing is performed, but if coarsening would be applied next, presmoothing does not take place on this grid. V_x and V_y are the semicoarsened grid V-cycles along the x- and y-directions. For instance, V_x can be described as follows.

$\mathrm{V}_x(A^{l_x,l_y}, f^{l_x,l_y}, \phi^{l_x,l_y}, \mu_1, \mu_2)$ {
if $(l_x = x(l_y))$ {
$\phi^{l_x,l_y} := S_z(A^{l_x,l_y}, f^{l_x,l_y}, \phi^{l_x,l_y}, \mu_1 + \mu_2);$
return ;
} ;
$\phi^{l_x,l_y} := S_z(A^{l_x,l_y}, f^{l_x,l_y}, \phi^{l_x,l_y}, \mu_1);$
$r^{l_x,l_y} := f^{l_x,l_y} - A^{l_x,l_y}\phi^{l_x,l_y};$
$f^{l_x-1,l_y} := R_x^{l_x,l_y} r^{l_x,l_y};$
$\phi^{l_x-1,l_y} := 0;$
$\mathrm{V}_x(A^{l_x-1,l_y}, f^{l_x-1,l_y}, \phi^{l_x-1,l_y}, \mu_1, \mu_2);$
$\phi^{l_x,l_y} = \phi^{l_x,l_y} + P_x^{l_x,l_y}\phi^{l_x-1,l_y};$
$\phi^{l_x,l_y} := S_z(A^{l_x,l_y}, f^{l_x,l_y}, \phi^{l_x,l_y}, \mu_2);$
}

Here the processed semicoarsened grids are $G^{l_x,l_y}, G^{l_x-1,l_y}, \ldots, G^{x(l_y),l_y}$. $x(l_y)$ is determined by the detection procedure according to the anisotropy of the matrix. S_z represents the z-line smoother. In the algorithm described above one smoothing step in MG-S involves $2(\mu_1 + \mu_2)$ relaxations on the standard grids.

Storage and computational complexity. In [12] it was shown that 2D MSG is still an $O(N)$-method, if a V- or an F-cycle is used. Since our variants process the same grids as in MSG, the same remark is also valid for the 2D MG-S. The total number of grid points to be stored for 2D standard multigrid is $\frac{4}{3}N$; for MG-S, it is $4N$. This can clearly be seen in Figure 7, where the additional grids are shown.

Next, we evaluate the computational complexity of the full MG-S cycle based on the relaxations on all grids. Here *full* MG-S means $x(l_y) = y(l_x) = 1$. Assuming a smoother on G^{m_x-l,m_y-l} with $(\frac{1}{4})^l N$ grid points in two dimensions requires $\xi(\frac{1}{4})^l N$ operations, the computational complexities C_V of the 2D V-cycle and C_F of our 2D F-cycle for standard multigrid and for MG-S are estimated as:

$$C_V = \left(1 + \frac{1}{4} + \frac{1}{16} + \frac{1}{64} + \ldots\right)(\nu_1 + \nu_2)\xi N = \frac{4}{3}(\nu_1 + \nu_2)\xi N, \tag{45}$$

$$C_F = \left(1 + \frac{1}{4} + \frac{2}{16} + \frac{3}{64} + \ldots\right)\nu_1\xi N + \left(1 + \frac{2}{4} + \frac{3}{16} + \frac{4}{64} + \ldots\right)\nu_2\xi N$$

$$= \left(\frac{13}{9}\nu_1 + \frac{16}{9}\nu_2\right)\xi N. \tag{46}$$

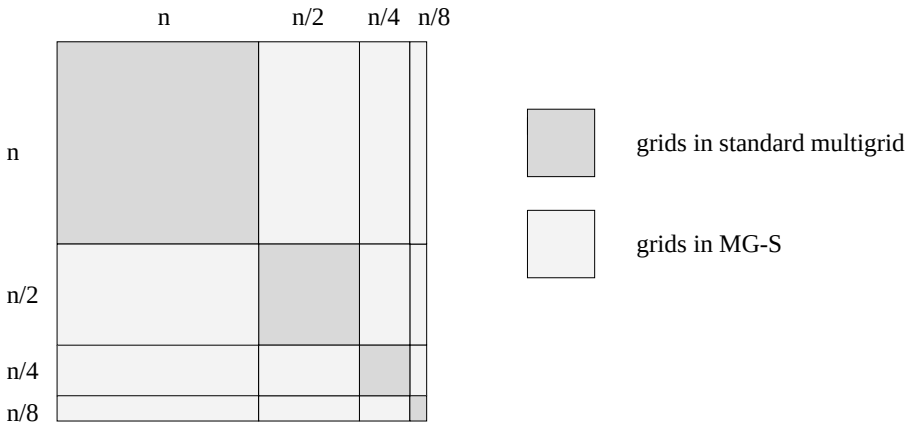

FIG. 7. *Storage and additional grids for standard multigrid and for* 2*D MG-S.*

The fact that less pre-work is done in our F-cycle is explained above. The difference between MG-S and standard multigrid is found in the operation count for the smoother. If we assume that one smoothing step inside a semicoarsened V-cycle requires η operations per grid point, we find for the alternating semicoarsened V-cycle smoother:

$$\xi(\mathrm{V}) = 2\eta(\mu_1 + \mu_2)\left(1 + \frac{1}{2} + \frac{1}{4} + \dots\right) = 4\eta(\mu_1 + \mu_2). \tag{47}$$

The computational complexity of the 2D alternating line smoother is estimated as:

$$\xi(AL) = 2\eta. \tag{48}$$

Hence, the 2D MG-S is approximately $2(\mu_1 + \mu_2)$ times as expensive as 2D standard multigrid with the alternating line smoother.

Since extra grids are not processed in the 3D MG-S method there is no additional storage, except for the third dimension. The number of points to be stored is then also $4N$. Furthermore, (45), (46), and (47) also hold for the estimations of the 3D MG-S method. This also implies that the MG-S F-cycle is still $O(N)$.

3*D smoother.* The parallelizable relaxation procedure is the damped four-color z-line Gauss–Seidel relaxation, with damping parameter $\omega = 0.8$. Here grid points are decomposed into four subsets :

$$\begin{aligned} C(1) &= \{(i,j,k) \mid i : \text{odd},\ j : \text{odd}\}, \\ C(2) &= \{(i,j,k) \mid i : \text{even},\ j : \text{odd}\}, \\ C(3) &= \{(i,j,k) \mid i : \text{odd},\ j : \text{even}\}, \\ C(4) &= \{(i,j,k) \mid i : \text{even},\ j : \text{even}\}. \end{aligned}$$

On each subset, a line solver is applied through all z-lines in parallel. The parallelization of the line smoother is described in more detail in [25].

Grid partitioning [10], [11], the usual way of parallelizing standard multigrid, is here used as the parallelization strategy for MG-S. The global grid is split into blocks, each assigned to a different process. The same block splitting is employed on all grids. Along the interior block boundaries the grid is stored with some overlap. Keeping the

values in overlap regions up-to-date on all multigrid levels requires communication between the nodes. A consequence of grid partitioning is that the grids in Figure 1(b) are processed sequentially.

3. 3D numerical results. Flexible MG-S used as a solver will be called a Richardson iteration here, for reasons explained before. Here we present the convergence results of the 3D flexible MG-S method as a preconditioner and as a solver. The results obtained are the number of iterations (n) needed to reduce the initial residual by eight orders of magnitude. Furthermore, the wall-clock time, T_w, in seconds on 48 processors on the Cenju-3 machine is presented. Regarding the detection of the strong couplings in section 2.4, we adopted 0.6 for δ_1 and δ_2 for all the problems in this section. We give the coarsest semicoarsened grid on each level to show which semicoarsened grids are processed in flexible MG-S. A full MG-S method for seven levels of (x,y)-coarsening would then have semicoarsened grids denoted by $(l_x, l_y) = (1,7), (1,6), \ldots, (1,2), (2,1), \ldots, (6,1), (7,1)$. The four problems solved in this subsection are thought to be "difficult" problems for multigrid solution methods and are in our opinion representative for a large class of problems.

Problem I: 3*D general anisotropic diffusion equation.* The first 3D test problem is a well-known test for robustness. The general anisotropic diffusion equation also tested in [24] and [5] looks like:

$$\begin{aligned} -a\phi_{xx} - b\phi_{yy} - c\phi_{zz} &= f \quad \text{on } \Omega = (0,1)^3, \\ \phi|_{x=0,y,z} = \phi|_{x,y=0,z} &= \phi|_{x,y,z=0} = 0, \\ \phi_n|_{x=1,y,z} = \phi_n|_{x,y=1,z} &= \phi_n|_{x,y,z=1} = 0. \end{aligned} \tag{49}$$

With coefficients a, b, and c, strong coupling of unknowns in one or two directions can be modeled. A robust solver must be able to solve (49) efficiently for all parameter sets. Representative parameter sets defined in [24] and also solved here are:

$$\begin{aligned} &\text{case 1:} \quad a \approx b \approx c \quad (a = b = c = 1), \\ &\text{case 2:} \quad a >> b \approx c \quad (a = 10^2, b = c = 1), \\ &\text{case 3:} \quad a \approx b >> c \quad (a = b = 10^2, c = 1), \\ &\text{case 4:} \quad a >> b >> c \; (a = 10^2, b = 1, c = 10^{-2}). \end{aligned} \tag{50}$$

In addition to the parameter sets in (50) another set is evaluated for each case. The relevant parameters are then evaluated once in the (x,y)-direction along the MG-S grids and once with one parameter in the z-direction, in order to show that robustness is assured with respect to a rotation of axes. In [24] it has been shown that for cases 3 and 4 standard multigrid with an alternating line smoother is not a satisfactory solver. In these cases a plane smoother is really necessary for convergence with standard multigrid. Table 1 presents the results for flexible MG-S as a solver and as a preconditioner for GMRES on a 75^3 grid with seven grid levels. The $\mathrm{V}(0,1)^{(0,1)}$-cycle already showed robust convergence for this test problem. The coarsest semicoarsened grids processed are also listed in this table.

Sometimes, the coarsening employed seems surprising; this is due to the lumping for the prolongation weights that is done in order to get the coarse grid matrices with a 27-point stencil. With a more severe detection criterion, choosing δ_i smaller, for some cases less solution iterations are needed, but then more grids are processed and the wall-clock time is larger. It is found that the solver can handle the general anisotropic

TABLE 1

Number of iterations (n) and T_w using the $\mathrm{V}(0,1)^{(0,1)}$-cycle of flexible MG-S as a solver and as a preconditioner for the general anisotropic diffusion equation on a 75^3 grid. Here no semicoarsening means that no strong couplings are detected along the semicoarsened direction.

Case	Parameters	Solution method	Cycle $\mathrm{V}(0,1)^{(0,1)}$	Coarsest grids
1	$a=b=c=1$	Richardson GMRES	(16) 11.9 (9) 5.3	x: (6,7), (1,4), (1,2) y: (7,6), (4,1), (2,1)
2	$a=b=1$, $c=10^2$	Richardson GMRES	(9) 6.1 (6) 4.8	x: (6,7) y: (7,6)
2	$a=c=1$, $b=10^2$	Richardson GMRES	(10) 8.2 (7) 6.6	No x-semicoarsening y: (7,3), (6,2), (5,2) (4,1), (3,1), (2,1)
3	$a=c=10^2$, $b=1$	Richardson GMRES	(12) 10.5 (8) 7.9	x: (3,7),(1,6), (1,5) (1,4), (1,3), (1,2) No y-semicoarsening
3	$a=b=10^2$, $c=1$	Richardson GMRES	(14) 9.5 (8) 6.2	x: (6,7) y: (7,6)
4	$a=1, b=10^2$ $c=10^{-2}$	Richardson GMRES	(10) 8.2 (8) 7.4	No x-semicoarsening y: (7,3),(6,2), (5,2) (4,1), (3,1),(2,1)
4	$a=10^2, b=10^{-2}$ $c=1$	Richardson GMRES	(13) 11.5 (9) 8.9	x: (1,7),(1,6), (1,5) (1,4), (1,3),(1,2) No y-semicoarsening

diffusion equation well for all parameter sets, as well as with the 3D flexible MG-S method as a solver and as a preconditioner. Grid-independent convergence rates (not shown) were found with very satisfactory wall-clock times. Also, the detection mechanism works well for this problem.

Problem II: *Poisson problem on a stretched grid.* The second problem investigated is the 3D Poisson equation on a grid with variable grid stretching. Our solvers are well suited for the solution of this kind of problems. The Poisson problem solved is:

$$-\phi_{xx} - \phi_{yy} - \phi_{zz} = 1 \ \text{ on } \ \Omega = (0,1)^3 \tag{51}$$

with the boundary conditions

$$\begin{aligned} \phi_n|_{x=0,y,z} = \phi_n|_{x,y=0,z} = \phi_n|_{x,y,z=0} = 0, \\ \phi_n|_{x=1,y,z} = \phi_n|_{x,y=1,z} = 0, \ \phi|_{x,y,z=1} = 0. \end{aligned} \tag{52}$$

ϕ_n is the derivative of ϕ in the normal direction, so we use Neumann boundary conditions on five boundary faces. A special stretched grid is chosen—a tensor product grid based on the Gauss–Lobatto–Legendre (GLL) points. GLL points provide an accumulation of grid points near the domain boundaries. In finite element literature the use of GLL grids is found to give nice properties for interpolation and integration, for example, for spectral elements. The interior grid points are computed as eigenvalues of the following matrix:

$$\begin{aligned} L_n &= [\mathrm{tridiag}(\gamma_{i-1}, 0, \gamma_i)] \ \text{ with} \\ \gamma_i &= \frac{1}{2}\sqrt{\frac{n(n+2)}{(n+\frac{1}{2})(n+\frac{3}{2})}}. \end{aligned} \tag{53}$$

Here n is the number of grid points in one dimension.

The grids investigated consist of 30^3, 60^3, and 75^3 grid points, and 6, 7, and 7 multigrid levels are used. Table 2 presents the results for the 3D flexible MG-S method used as a solver and as a preconditioner. Results are presented for the $\mathrm{V}(1,1)^{(0,1)}$- and $\mathrm{F}(1,1)^{(0,1)}$-cycles. It is interesting to see which grids are chosen by the flexible MG-S preconditioner in the presence of variable stretched grid cells. Here, the coarsest grids for the 75^3 problem were: (5,7), (5,6), (4,5), (3,4), (1,3), (1,2) for x-semicoarsening and the symmetric counterparts for y-semicoarsening. The multigrid F-cycle solvers show a very satisfactory level-independent performance. The use of MG-S as a preconditioner is more robust with respect to the choice of cycle for this problem.

TABLE 2
Number of iterations (n) and T_w using $\mathrm{V}(1,1)^{(0,1)}$ and $\mathrm{F}(1,1)^{(0,1)}$ cycles of 3D flexible MG-S as a solver and as a preconditioner for the Poisson equation on several GLL grids.

Grid	Solver	Cycle	
		$\mathrm{V}(1,1)^{(0,1)}$	$\mathrm{F}(1,1)^{(0,1)}$
30^3	Richardson	(15) 4.6	(10) 5.4
	GMRES(20)	(9) 3.1	(8) 4.9
60^3	Richardson	(19) 18.7	(10) 15.3
	GMRES(20)	(9) 9.9	(7) 12.2
75^3	Richardson	(19) 34.7	(10) 30.1
	GMRES(20)	(10) 20.4	(8) 27.1

It can be concluded that for this kind of Poisson problem, the flexible MG-S method with the F-cycle used as a solver already produces very satisfactory results; the Krylov acceleration does not improve the convergence considerably, but (more important) also does not increase wall-clock times.

Problem III: *Convection-diffusion equation with spherical solution.* The third problem evaluated is a 3D convection-diffusion problem, where all directions appear in the convection terms, with Dirichlet boundary conditions:

$$\begin{aligned} -\epsilon\Delta\phi + a(x,y,z)\phi_x + b(x,y,z)\phi_y + c(x,y,z)\phi_z &= 1 \ \text{ on } \Omega = (0,1)^3, \\ \phi &= f(x,y,z) \ \text{ on } \partial\Omega, \end{aligned} \tag{54}$$

with

$$\begin{aligned} a(x,y,z) &= -2\cos(\pi x)\cos(\pi y)\sin(\pi z), \\ b(x,y,z) &= \sin(\pi x)\cos(\pi y)\cos(\pi z), \\ c(x,y,z) &= \cos(\pi x)\sin(\pi y)\cos(\pi z), \text{ and} \\ f(x,y,z) &= \sin(\pi x) + \sin(13\pi x) + \sin(\pi y) + \sin(13\pi y) + \sin(\pi z) + \sin(13\pi z). \end{aligned}$$

The convection terms are discretized with a standard first-order upwind discretization. A convection-dominated test case is chosen with $\epsilon = 10^{-6}$. The solution obtained on a 17^3 grid is presented in Figure 8(a). Table 3 presents the results for 3D flexible MG-S used as a solver and as a preconditioner. For this problem the full 3D MG-S grid sequence was detected for processing. The iteration cycles compared are $\mathrm{V}(0,1)^{(0,1)}$ and $\mathrm{F}(0,1)^{(0,1)}$.

In Table 3 it can be seen that the number of iterations of the flexible MG-S as a solver increases with the number of grid points. However, this grid dependence is considerably improved by the Krylov acceleration.

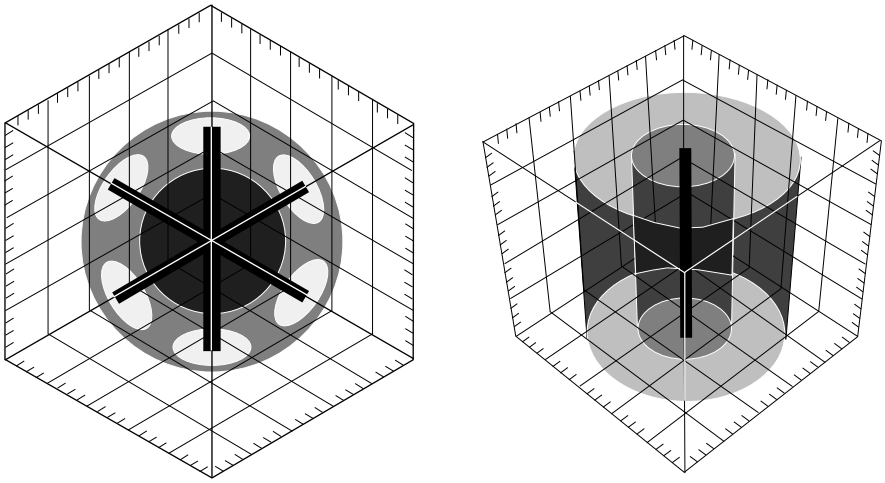

(a) (b)

FIG. 8. *Spherical and cylindrical solutions of convection-diffusion Problems III and IV,* 17^3 *grid.*

TABLE 3
Number of iterations (n) *and* T_w *using* $\mathrm{V}(0,1)^{(0,1)}$ *and* $\mathrm{F}(0,1)^{(0,1)}$ *cycles of 3D flexible MG-S as a solver and as a preconditioner for the convection-diffusion equation* (54) *on several grids.*

Grid	Solver	Cycle	
		$\mathrm{V}(0,1)^{(0,1)}$	$\mathrm{F}(0,1)^{(0,1)}$
30^3	Richardson	(26) 8.7	(26) 17.7
	GMRES(20)	(15) 5.4	(14) 10.1
60^3	Richardson	(46) 39.2	(45) 74.1
	GMRES(20)	(22) 20.9	(20) 35.0
75^3	Richardson	(67) 88.3	(41) 97.4
	GMRES(20)	(24) 35.0	(20) 50.7

Problem IV: *Convection-diffusion equation with cylindrical solution.* In the next 3D convection-diffusion problem two directions appear in the convection terms. In equation (54) functions $a, b, c,$ and f are now chosen as:

$a(x,y,z) = \sin(\pi x)\cos(\pi y),$
$b(x,y,z) = -\cos(\pi x)\sin(\pi y),$
$c(x,y,z) = 10^{-5}z,$
$f(x,y,z) = \sin(\pi x) + \sin(13\pi x) + \sin(\pi y) + \sin(13\pi y) + 10^{-5}z.$

The convection terms are discretized with a standard upwind discretization. A convection-dominated test case is chosen with $\epsilon = 10^{-6}$. It was found that this choice of $c(x,y,z)$ represented the hardest test case for our solver; larger choices of $c(x,y,z)$ like $c = z$ showed much faster convergence. The obtained solution on a 17^3 grid is shown in Figure 8(b). Table 4 presents the convergence results for this problem. The $\mathrm{V}(0,1)^{(0,1)}$-cycle is used, and all the semicoarsened grids are processed.

The MG-S-based solvers also perform very satisfactorily for this problem. With a rotation of axes convergence slows down somewhat for this problem, but the results with GMRES are still satisfactory. It can be concluded that for convection-dominated problems the GMRES acceleration considerably improves convergence and wall-clock times.

TABLE 4
Number of iterations (n) and T_w using $\mathrm{V}(0,1)^{(0,1)}$ cycles of 3D flexible MG-S as a solver and as a preconditioner for the convection-diffusion equation with cylindrical solution.

Grid	Solver	Cycle
		$\mathrm{V}(0,1)^{(0,1)}$
30^3	Richardson	(15) 4.3
	GMRES(20)	(12) 3.8
60^3	Richardson	(22) 17.0
	GMRES(20)	(15) 12.7
75^3	Richardson	(26) 32.1
	GMRES(20)	(15) 20.1

4. Conclusion. We present a robust 3D multigrid-based solver with a flexible MG-S preconditioner for the Krylov subspace method GMRES. The method is specially suited for problems arising from block-structured applications and finite volume or finite difference discretizations. The flexibility of processing only certain grids in multiple semicoarsening methods without losing the robustness further reduces the wall-clock times for this kind of method. In particular, the use of the flexible MG-S method as a preconditioner was found to be robust with respect to the choice of the iteration cycle, the number of smoothing steps, and the damping parameter. The method presented is a very satisfactory alternative for achieving robustness for standard multigrid methods with alternating plane smoothers.

Acknowledgment. The fruitful discussions with Ulrich Trottenberg, Yair Shapira, and Bernhard Hientzsch are gratefully acknowledged, as is the correction of the English text by Robin Calkin. The authors also wish to thank referees for their useful comments and careful reading of the manuscript.

REFERENCES

[1] A. BRANDT, *Multi-level adaptive solutions to boundary-value problems*, Math. Comp., 31 (1977), pp. 333–390.
[2] J. E. DENDY, JR., *Black box multigrid*, J. Comput. Phys., 48 (1982), pp. 366–386.
[3] J. E. DENDY, JR., *Two multigrid methods for three-dimensional problems with discontinuous and anisotropic coefficients*, SIAM J. Sci. Stat. Comput., 8 (1987), pp. 673-685.
[4] J. E. DENDY, JR. AND C. C. TAZARTES, *Grandchild of the frequency domain multigrid method*, SIAM J. Sci. Comput., 16 (1995), pp. 307–319.
[5] U. GÄRTEL, A. KRECHEL, A NIESTEGGE, AND H.-J. PLUM, *Parallel multigrid solution of 2D and 3D anisotropic elliptic equations: Standard and nonstandard smoothing*, in Multigrid Methods III, Internat. Ser. Numer. Math. 98, W. Hackbusch and U. Trottenberg, eds., Birkhäuser, Basel, Switzerland, 1991, pp. 191–209.
[6] W. HACKBUSCH, *Multi-Grid Methods and Applications*, Springer-Verlag, Berlin, Germany, 1985.
[7] W. HACKBUSCH, *The frequency domain decomposition multigrid method, Part* I: *Application to anisotropic equations*, Numer. Math., 56 (1989), pp. 229–245.
[8] R. HEMPEL, R. CALKIN, R. HESS, W. JOPPICH, U. KELLER, N. KOIKE, C. W. OOSTERLEE, H. RITZDORF, T. WASHIO, P. WYPIOR, AND W. ZIEGLER, *Real applications on the new parallel system NEC Cenju-*3, Parallel Comput., 22 (1996), pp. 131–148.
[9] R. KETTLER, *Analysis and comparison of relaxation schemes in robust multigrid and preconditioned conjugate gradient methods*, in Multigrid Methods, Lecture Notes in Math. 960, W. Hackbusch and U. Trottenberg, eds., Springer-Verlag, Berlin, Germany, 1982, pp. 502–534.
[10] J. LINDEN, B. STECKEL, AND K. STÜBEN, *Parallel multigrid solution of the Navier-Stokes equations on general 2D-domains*, Parallel Comput., 7 (1988), pp. 461-475.
[11] O. A. MCBRYAN, P. O. FREDERICKSON, J. LINDEN, A. SCHÜLLER, K. SOLCHENBACH, K. STÜBEN, C. A. THOLE, AND U. TROTTENBERG, *Multigrid methods on parallel computers - a survey of recent developments*, Impact Comput. Sci. Engrg., 3 (1991), pp. 1–75.

[12] W. A. Mulder, *A new multigrid approach to convection problems*, J. Comput. Phys., 83 (1989), pp. 303–323.
[13] N. H. Naik and J. van Rosendale, *The improved robustness of multigrid elliptic solvers based on multiple semicoarsened grids*, SIAM Numer. Anal., 30 (1993), pp. 215–229.
[14] C. W. Oosterlee and P. Wesseling, *On the robustness of a multiple semi-coarsened grid method*, Z. Angew. Math. Mech., 75 (1995), pp. 251–257.
[15] C. W. Oosterlee, *The convergence of parallel multiblock multigrid methods*, Appl. Numer. Math., 19 (1995), pp. 115–128.
[16] C. W. Oosterlee, *A GMRES-based plane smoother in multigrid to solve three-dimensional anisotropic fluid flow problems*, J. Comput. Phys., 130 (1997), pp. 41–53.
[17] C. W. Oosterlee and T. Washio, *An evaluation of parallel multigrid as a solver and a preconditioner for singular perturbed problems*, SIAM J. Sci. Comput., 19 (1998), to appear.
[18] M. Ries, U. Trottenberg, and G. Winter, *A note on MGR methods*, Linear Algebra Appl., 49 (1983), pp. 1–26.
[19] J. Ruge and K. Stüben, *Algebraic multigrid (AMG)*, in Multigrid Methods, Frontiers in Appl. Math. 5, S. McCormick, ed., SIAM, Philadelphia, 1987, pp. 73–130.
[20] Y. Saad and M.H. Schultz, *GMRES: A generalized minimal residual algorithm for solving nonsymmetric linear systems*, SIAM J. Sci. Comp., 7 (1986), pp. 856–869.
[21] Y. Saad, *Preconditioned Krylov subspace methods for CFD application,* in Proceedings of the Internat. Workshop on Solution Techniques for Large-Scale CFD Problems, W. G. Habashi, ed., Cerca, Montréal, Québec, Canada, 1994.
[22] Y. Shapira, M. Israeli, and A. Sidi, *Towards automatic multigrid algorithms for SPD, non-symmetric and indefinite problems*, SIAM J. Sci. Comput., 17 (1996), pp. 439–453.
[23] R. A. Smith and A. Weiser, *Semicoarsening multigrid on a hypercube*, SIAM J. Sci. Comput., 13 (1992), pp. 1314–1329.
[24] C. A. Thole and U. Trottenberg, *Basic smoothing procedures for the multigrid treatment of elliptic* 3*-D operators*, Appl. Math. Comp., 19 (1986), pp. 333–345.
[25] T. Washio and C. W. Oosterlee, *Experiences with Robust Parallel Multilevel Preconditioners for BiCGSTAB*, GMD Arbeitspapier 949, GMD St. Augustin, Germany, 1995.
[26] P. Wesseling, *An Introduction to Multigrid Methods*, John Wiley, Chichester, UK, 1992.
[27] P. M. de Zeeuw, *Matrix-dependent prolongations and restrictions in a blackbox multigrid solver*, J. Comp. Appl. Math., 33 (1990), pp. 1–27.
[28] P.M. de Zeeuw, *Development of semi-coarsening techniques*, Appl. Numer. Math., 19 (1996), pp. 433-465.